Characteristics of multivalent impurity doped C_{60} films grown by MBE

Jiro Nishinaga[1,2], Tomoyuki Aihara[1,2], Atsushi Kawaharazuka[3], Yoshiji Horikoshi[1,2]

[1]School of Science and Engineering, Waseda University, 3-4-1 Okubo, Shinjuku-ku, Tokyo 169-8555, Japan

[2]Kagami Memorial Laboratory for Materials Science and Technology, Waseda University, 2-8-26 Nishiwaseda, Shinjuku-ku, Tokyo 169-0051, Japan

[3]Consolidated Research Institute for Advanced Science and Medical Care, Waseda University, 513 Waseda-Tsurumaki-cho, Shinjuku-ku, Tokyo 162-0041, Japan

Phone: +81-3-5286-3176, FAX: +81-3-3209-3450

E-Mail: jiro247@moegi.waseda.jp

Abstract

Metal-doped C_{60} films (aluminum, gallium and germanium) are grown on GaAs and quartz glass substrates by solid source molecular beam epitaxy. Mechanical and optical properties of the films are investigated by Vickers hardness test and photoluminescence measurement. Vickers hardness values of all the impurity doped C_{60} films are considerably enhanced. Photoluminescence peaks of the electron transition between HOMO and LUMO states of C_{60} molecules are confirmed in Al-doped and Ga-doped C_{60} films, but not in Ge-doped C_{60} films. Optimized bonding structures of these impurity atoms to C_{60} molecules are determined by using ab initio calculations. Stable covalent bonds between impurities and C_{60} molecules are verified to be formed. The impurity atoms may act as bridges between C_{60} molecules. The distortion of C_{60} cages due to the bonding with metals is confirmed. In the Al and Ga-doped C_{60} films, this distortion probably make the dipole forbidden transition relieved. The binding energies are found to be related to the experimentally determined Vickers hardness.

PACS codes: 61.48.+c; 62.20.-x; 68.43.Bc; 78.55.Kz

Keywords: A1. Computer simulation; A1. Doping; A1. Photoluminescence; A3. Molecular Beam Epitaxy; B1. Fullerenes; B1. Organic compounds

1. Introduction

Variety of investigations have been done for the physical and chemical properties of C_{60}, and revealed unique potentialities of C_{60} such as superconductivity [1] and photoconductivity [2] materials. C_{60} has also been applied to a cluster ion source material [3]. However, C_{60} crystals are very fragile and chemically unstable due to the fact that C_{60} crystals are formed by the van der Waals force, which is very weak compared with other bonding structures such as covalent and ionic bindings [4]. Thus, the films are not suitable for practical device applications. To investigate the feasibility of C_{60} layers, it is inevitable to obtain harder and more stable C_{60} films, keeping the original characteristics of C_{60} films. It has been reported that the metal-C_{60} interaction is stronger than C_{60}-C_{60} van der Waals interaction [5, 6]. Therefore, it is expected that metal doping in C_{60} films produces much harder and chemically stable C_{60} films. We have shown that aluminum doping is very effective to make C_{60} films much harder and more stable, and the parity forbidden transition between the highest occupied molecular orbital (HOMO) and the lowest unoccupied molecular orbital (LUMO) is relieved [7]. These characteristics are probably caused by the bonding between aluminum and C_{60}.

In this paper, C_{60} layers doped with multivalent impurities such as aluminum, gallium and germanium are grown on GaAs substrates and quartz glass substrates by MBE and their mechanical and optical properties are investigated. Vickers hardness test is used to evaluate the mechanical properties of the films, and photoluminescence (PL) measurement is used to study the optical properties. In order to obtain optimized structures and the corresponding binding energies between these impurities and C_{60} molecules, ab initio calculations are performed. As a result, stable covalent bonds are verified to be formed between them. The binding energies are confirmed to be much higher than that of the van der Waals force between C_{60} molecules.

2. Experimental procedure

Metal-doped C_{60} films are grown on GaAs (001) and quartz glass substrates by solid source MBE with background pressure of 10^{-10} Torr. GaAs substrates are first etched in an alkaline etchant, and loaded in the growth chamber. Native oxide layers of GaAs surfaces are removed by a thermal flash at 580°C in As_4 atmosphere. After growing a 50-nm-thick GaAs buffer layer at 580°C, metal-doped C_{60} film growth is performed at a substrate temperature of 100°C. 99.5% C_{60} powder is used as the C_{60} source. The beam equivalent pressure of C_{60} is fixed at 1.0×10^{-7} Torr with the deposition rate of 0.23Å/sec. The impurity cell temperatures (Al, Ga, Ge) are varied to control the molecular ratios of metal atoms to C_{60} molecules. The stacking coefficients of metal impurities are assumed to be unity, because the substrate temperature is as low as 100°C. The sticking coefficient of C_{60}

should be also unity because the growth rate of C_{60} layers at substrate temperatures below 150°C remains constant. Therefore, the resulting compositions of the grown layers are equal to the flux ratios. Table 1 shows the cell temperatures of the impurities with different flux ratios of metal atoms to C_{60} molecules.

Quartz glass substrates are degreased by an organic solvent and the surface contaminations are evaporated by a thermal anneal at 600°C for 30 minutes in the growth chamber before deposition. Metal-doped C_{60} films are grown on the same manner as those grown on GaAs substrates.

The crystalline properties are investigated by reflection high energy electron diffraction (RHEED) and X-ray diffraction (XRD) $2\theta/\omega$ scan. Vickers hardness test is applied to investigate the mechanical properties. PL measurement is performed at room temperature by using the 488 nm line of argon ion laser as an excitation source.

3. Results and discussion

Pure C_{60} films crystallize into a face-centered cubic on Si and GaAs substrates [8, 9, 10]. However, all the impurity doped C_{60} films on both GaAs and quartz glass substrates show halo RHEED patterns from the beginning of the growth, and the films show no distinct peak in XRD $2\theta/\omega$ scan, indicating that the C_{60} films doped with these impurity atoms have amorphous structures.

The Vickers hardness value of pure C_{60} crystals is reported to be around 20HV [11, 12], which is equal to that of pure gold surfaces. Table 2 shows the Vickers hardness of pure

C_{60} and impurity doped C_{60} films. The Vickers hardness of the impurity doped C_{60} films is confirmed to be increased. Especially, the value of Ge-doped C_{60} films is as high as 450HV, which is approximately equal to the value of plated nickel surfaces. The order of the Vickers hardness is Ge-doped C_{60} > Al-doped C_{60} > Ga-doped C_{60}, and this order should be closely related to the binding energies between impurities and C_{60} molecules.

Pure C_{60} crystals are quickly dissolved in organic solvents due to the weak binding energy of C_{60} crystals. On the other hand, all the impurity doped C_{60} films are found to be undissolved in organic solvents. The structural changes and the hardness enhancements are probably induced by the bonding between C_{60} molecules and multivalent metal atoms. As a result, the impurity atoms may act as bridges between C_{60} molecules. They make large-scale complexes, and these complexes connect firmly with each other.

PL spectra of the pure, Al-doped and Ga-doped C_{60} films grown on quartz glass substrates are shown in Fig. 1. The measurements are performed at room temperature. The PL spectrum of the pure C_{60} is in good agreement with the results in the literatures [13, 14]. The most dominant emission line in pure C_{60} films (peak 2) lies around 1.69eV, which is attributed to a radiative recombination of a self-trapped polaron exciton. The peak 1 (1.50eV) is considered to be a phonon replica of the peak 2. This vibrational mode corresponds to the A_g mode phonon peak in Raman spectrum at 1469cm^{-1}. In the Al-doped and Ga-doped C_{60} films, additional PL peaks appear around 1.75eV (peak 3), 1.85eV (peak 4) and 1.95eV (peak 5). In pure C_{60} crystals, the electron transition between HOMO and

LUMO is parity forbidden [4]. The energy of the peak 5 coincides well with the energy difference between HOMO and LUMO states, indicating that the parity forbidden transition is relieved by the metal-C_{60} bonding. The peak 3 and peak 4 are considered to be the phonon replicas of peak 5. The spectra suggest that the aluminum doping enhances the radiative recombination between HOMO and LUMO states more effectively.

Fig. 2 shows PL spectra of the pure and Ge-doped C_{60} films grown with several molecular ratios measured at room temperature. These spectra show that the luminescence from C_{60} molecules is considerably suppressed as a result of the Ge-C_{60} interactions.

To investigate the bonding characters between these impurity atoms and C_{60} molecules, the configurations of the impurity atoms and C_{60} molecules are optimized by using the Gaussian 03 computer software [15] for the B3LYP molecular calculations. Fig. 3 shows the optimized topography with the electron density of C_{60}-Ge-C_{60} system. This result suggests that the electrons are shared between Ge and C_{60} molecules, indicating that stable covalent bonds are formed between them. The stable covalent bonds between the other impurity atoms and C_{60} molecules are confirmed in the same manner. The binding energies between impurities and C_{60} molecules are estimated by evaluating the energies of the complexes, and then subtracting those of the individual impurity atoms and C_{60} molecules. Table 3 shows the calculated binding energies in one metal and one C_{60} molecule system. The binding energies are confirmed to be much higher than that of the van der Waals force between C_{60} molecules [16, 17]. The order of the binding energies in Table 3 (Ge-doped C_{60}

> Al-doped C_{60} > Ga-doped C_{60}) coincides well with that of the experimentally obtained Vickers hardness. Thus, the Vickers hardness improvement by multivalent impurity doping is qualitatively confirmed.

Fig. 4 shows the optimized structure of an aluminum atom and a C_{60} molecule system (a), and that of a germanium atom and a C_{60} molecule system. In order to compare the distortion induced by the bonding with the metal atom, the magnified images with the carbon atoms bonding structure of a pure C_{60} cage are shown in the insets. Discernible differences can be observed between Al-C_{60} and Ge-C_{60} systems. Bearing the above calculation results in mind, the experimentally obtained PL date may be explained by the following hypothesis: In Al-C_{60} system, the distortion of the C_{60} cage is found to be very little, and then the weak distortion may make the dipole forbidden transition relieved. On the other hand, the distortion of the C_{60} cage induced by the Ge-C_{60} bonding is confirmed to be enhanced. This distortion is probably strong enough to suppress the radiative recombination of C_{60} molecules.

4. Conclusions

Metal-doped C_{60} films are fabricated on GaAs and quartz glass substrates by solid source MBE and the binding energies between metal atoms and C_{60} molecules are calculated by ab initio calculations. The RHEED exhibits halo patterns and all the films show no distinct peak in XRD $2\theta/\omega$ scan. The Vickers hardness values of all the impurity doped C_{60} films are confirmed to be enhanced, and the order of the Vickers hardness is Ge-doped

C_{60} > Al-doped C_{60} > Ga-doped C_{60}. The PL peak between HOMO and LUMO states of C_{60} is confirmed in the Al-doped and Ga-doped C_{60} films. Optimized structures of impurity atoms to C_{60} molecules are calculated. Stable covalent bonds between impurities and C_{60} molecules are confirmed to be formed. The impurity atoms probably act as bridges between C_{60} molecules. In Al and Ga-doped C_{60} films, the distortion may make the dipole forbidden transition relieved. The distortion between Ge and C_{60} is probably strong enough to suppress the radiative recombination of C_{60} molecules. The order of the binding energies between them coincides well with that of the experimentally obtained Vickers hardness.

Acknowledgements

This work is partly supported by 21st century COE “Practical Nano-Chemistry” from the Ministry of Education, Science, Sports and Culture, Japan, and by the Grant-in-aid for Scientific Research (A) (17206031) from Japan Society for the Promotion of Science (JSPS).

References

[1] A.F. Hebard, M.J. Rosseinsky, R.C. Haddon, D.W. Murphy, S.H. Glarum, T.T.M. Palstra, A.P. Ramirez, A.R. Kortan, Nature 350 (1991) 600.

[2] Y. Wang, Nature 356 (1992) 585

[3] D. Weibel, S. Wong, N. Lockyer, P. Blenkinsopp, R. Hill, J.C. Vickerman, Anal. Chem.75 (2003) 1754.

[4] S. Saito, A. Oshiyama, Phys. Rev. Lett. 66 (1991) 2637.

[5] A.V. Hamza, J. Dykes, W.D. Mosley, L. Dinh and M. Balooch, Surface Science. 318 (1994) 368.

[6] A.J. Maxwell, P.A. Brühwiler, D. Arvanitis, J. Hasselström, M.K.J. Johansson and N. Martensson, Phys. Rev. B. 57 (1998) 7312.

[7] J. Nishinaga, T. Aihara, H. Yamagata, Y. Horikoshi, J. Cryst. Growth 278 (2005) 633.

[8] J. Nishinaga, M. Ogawa, Y. Horikoshi, Thin Solid Films 464-465 (2004) 323.

[9] J. Nishinaga, T. Aihara, T. Toda, F. Matsutani, Y. Horikoshi, J. Vac. Sci. Technol. B 24 (2006) 1587.

[10] W.M. Tong, D.A.A. Ohlberg, H.K. You, R.S. Williams, S.J. Anz, M.M. Alvarez, R.L. Whetten, Y. Rubin, F.N. Diederich, J. Phys. Chem. 95 (1991) 4709.

[11] J. Li, S. Komiya, T. Tamura, C. Nagasaki, J. Kihara, K. Kishio, K. Kitazawa, Physica C 195 (1992) 205.

[12] M. Tachibana, M. Michiyama, K. Kikuchi, Y. Achiba, K. Kojima, Phys. Rev. B. 49 (1994) 14945.

[13] V. Capozzi, G. Casamassima, G.F. Lorusso, A. Minafra, R. Piccolo, T. Trovato A. Valentini, Solid State Commun. 98 (1996) 853.

[14] I. Akimoto, K. Kan’no, J. Phys. Soc. Jpn. 71 (2002) 630.

[15] M.J. Frisch et al., Gaussian 03, Revision C.02, Gaussian Inc., Wallingford, CT, 2004.

[16] L.A. Girifalco, J. Phys. Chem. 96 (1992) 858.

[17] P.A. Gravil, M. Devel, Ph. Lambin, X. Bouju, Ch. Girard, A.A. Lucas, Phys. Rev. B, 53

(1996) 1622.

Figure Captions

Fig. 1. Photoluminescence spectra of pure C_{60} and impurity (Al, Ga) doped C_{60} films grown on quartz glass substrates with a molecular ratio of metal atoms to C_{60} molecules of 25 measured at room temperatures.

Fig. 2. Photoluminescence spectra of pure C_{60} and Ge-doped C_{60} films with the several molecular ratios of metal atoms to C_{60} molecules grown on quartz glass substrates measured at room temperatures.

Fig. 3. Optimized topography with the electron density of C_{60} - Ge - C_{60} system.

Fig. 4. Optimized structures of an aluminum atom and a C_{60} molecule system (a), and a germanium atom and a C_{60} molecule system. In these insets, the magnified images with the carbon atoms bonding structures of pure C_{60} cage are shown.

Table 1. Cell temperatures with different ratios of metal to C_{60}.

Flux ratios of metal to C_{60}	3	10	25
Ga cell temperature (°C)	710	755	805
Al cell temperature(°C)	985	1075	1130
Ge cell temperature(°C)	1070	1150	1190

Table 2. Vickers hardness values of pure and metal doped C_{60} films.

Pure C_{60} crystals	Ga-doped C_{60} films (Ga / C_{60}=25)	Al-doped C_{60} films (Al / C_{60}=25)	Ge-doped C_{60} films (Ge / C_{60}=25)
20HV*	70HV0.01	245HV0.01	450HV0.01

*Reference data [11, 12]

Table 3. Binding energies between a metal atom and a C_{60} molecule.

system	B3LYP / 6-311+G(d) // B3LYP / 6-31G
C_{60} - C_{60}	0.24 eV*
C_{60} - Ga	0.83 eV
C_{60} - Al	0.96 eV
C_{60} - Ge	1.22 eV

*Reference data [16, 17]

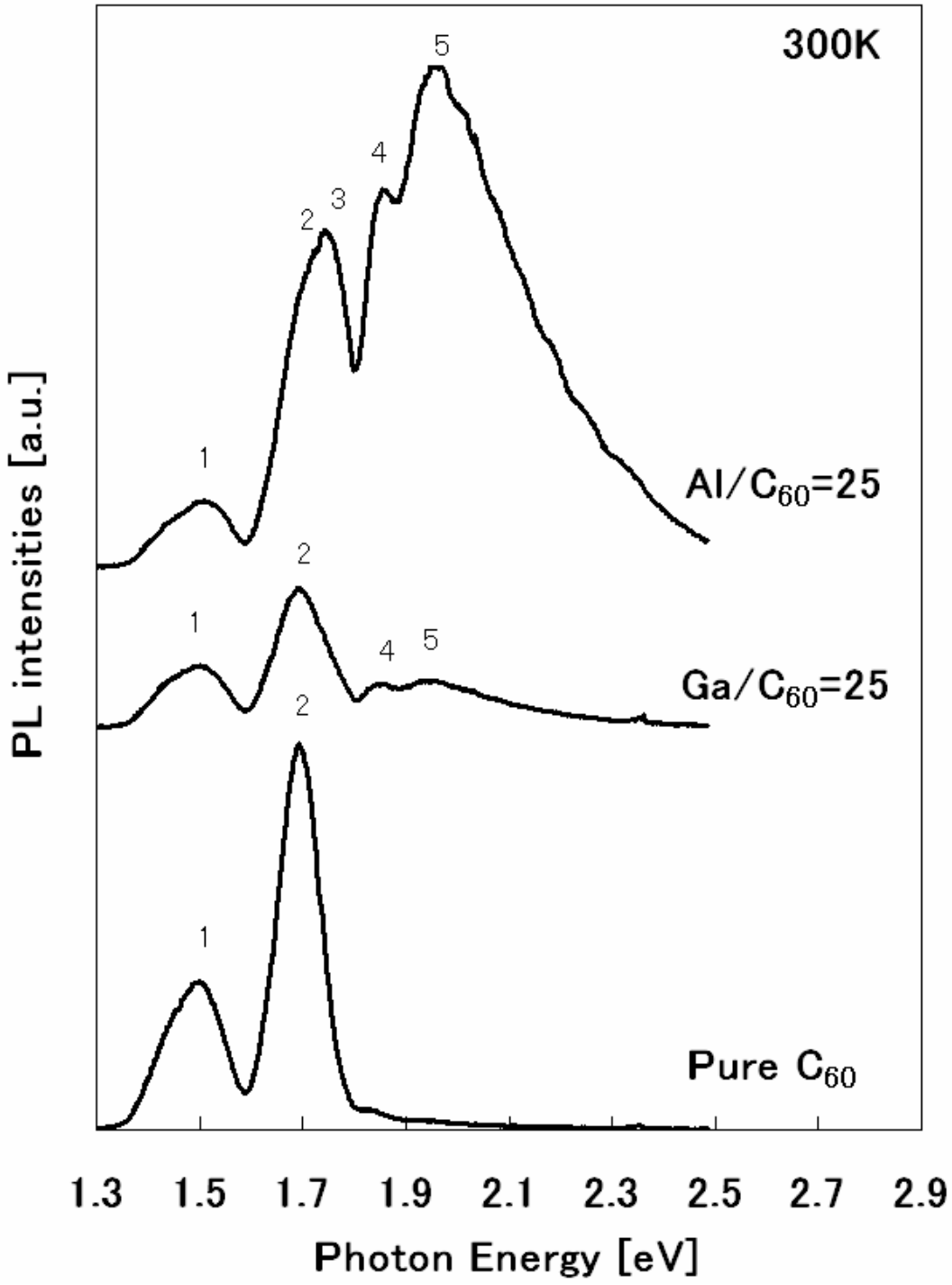
300K
5
4
2
3
1
Al/C60=25
2
1
4
5
Ga/C60=25
2
1
Pure C60
PL intensities [a.u.]
1.3
1.5
1.7
1.9
2.1
2.3
2.5
2.7
2.9
Photon Energy [eV]

Fig. 1

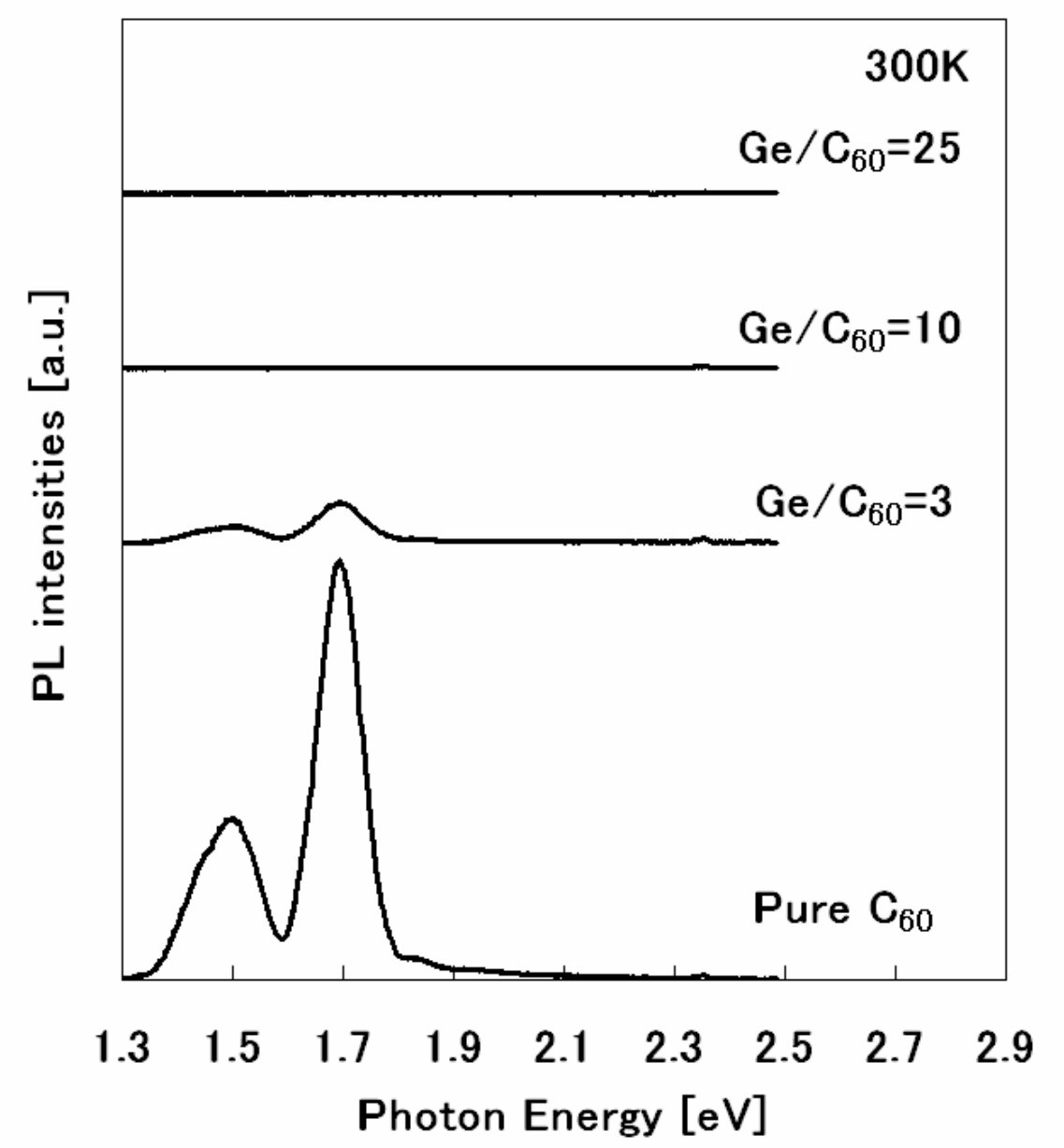
300K
Ge/C60=25
Ge/C60=10
Ge/C60=3
Pure C60
PL intensities [a.u.]
1.3
1.5
1.7
1.9
2.1
2.3
2.5
2.7
2.9
Photon Energy [eV]

Fig. 2

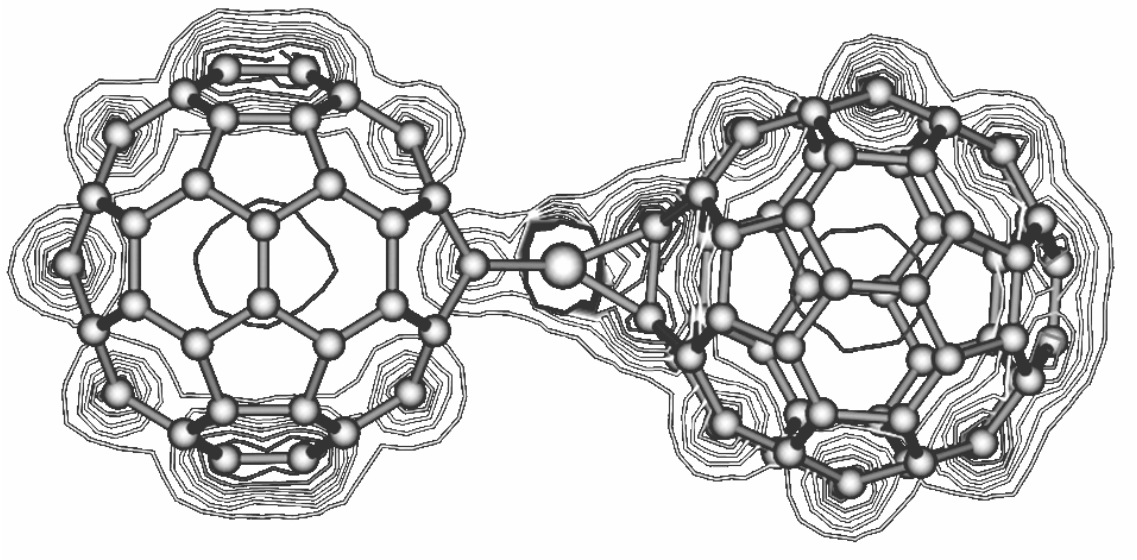

Fig. 3

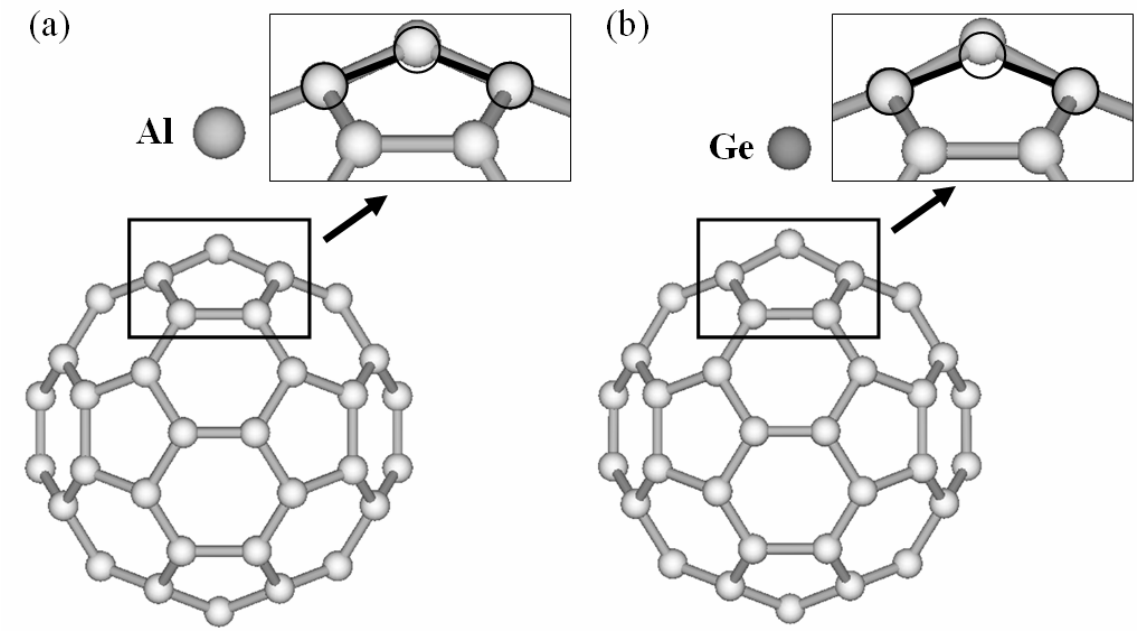

Fig. 4